Electronic Supplementary Information

A "turn-on" lanthanide complex chemosensor for recognition of lead(II) based on the formation of nanoparticles

Benhua Xu,[a] Xiaoliang Tang,[a] Ji'an Zhou,[a] Wanmin Chen,[a] Haile Liu,[a] Zhenghua Ju[a] and Weisheng Liu*[a]*

[a] Key Laboratory of Nonferrous Metal Chemistry and Resources Utilization of Gansu Province and State Key Laboratory of Applied Organic Chemistry, Key Laboratory of Special Function Materials and Structure Design, Ministry of Education, College of Chemistry and Chemical Engineering, Lanzhou University, Lanzhou, 730000, China

***** Corresponding authors:
E-mail for X. Tang: *tangxiaol@lzu.edu.cn*; E-mail for W. Liu: *liuws@lzu.edu.cn*
Fax: +86-931-8912582

1. Synthesis.

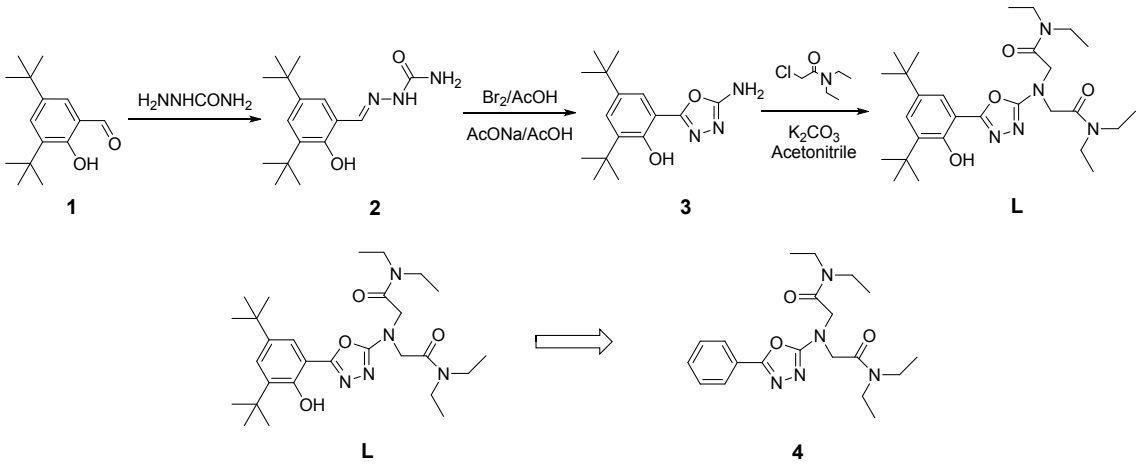

Scheme S1 The synthesis of the target ligand **L** and similar ligand **4**

Compound **2** and **3** are synthesized according to our previous work.[1]

Ligand **4** as white powder was prepared in the same way except that benzaldehyde was used instead of 3,5-Bis(1,1-dimethylethyl)-2-hydroxy-benzaldehyde **1**. Yield: 87.0 %. ^{1}H NMR (400 MHz, $CDCl_3$): δ = 7.82–7.85 (2H, m, Ar-H), 7.41–7.43 (3H, m, Ar-H), 4.53 (4H, s, -CH_2-), 3.41 (4H, q, J = 7.2 Hz, -CH_2-), 3.36 (4H, q, J = 7.2 Hz, -CH_2-), 1.27 (6H, t, J = 7.2 Hz, -CH_3), 1.14 (6H, t, J = 7.2 Hz, -CH_3); ^{13}C NMR (100 MHz, $CDCl_3$): δ = 167.02, 164.39, 159.21, 130.41, 128.84, 125.75, 124.74, 50.07, 41.45, 40.69, 14.39, 13.14; ESI-MS *m/z* [$(M+H)^+$]: 388.2099.

Chemosensor compound (Tb-2):

Complex **Tb-2** was prepared in the same way as complex **Tb-1** except that ligand **4** was used instead of **L**. The colorless complex crystals were collected and dried to afford **Tb-2**. Yield: 65 %. IR (KBr, cm^{-1}): 3438(m), 2985(w), 1635(s), 1613(s), 1561(w), 1485(s), 1384(m), 1315(m), 1276(m), 1212(w), 1152(w), 1103(w), 1075(w), 1027(w), 953(w), 903(w), 814(w), 777(w), 745(w), 729(w), 693(w).

2. Crystal Data.

Table S1 Crystal Data and Structural Refinement Parameters for Complexes.

	Tb-1	**Tb-2**
Formula	$C_{32}H_{55}N_8O_{16}Tb$	$C_{20}H_{31}N_8O_{13}Tb$
CCDC Number	1455764	1455765
Formula Weight	966.76	750.45
Crystal System	Monoclinic	Triclinic
Space Group	$P2_1/c$	$P\bar{1}$
a (Å)	10.311 (5)	9.520 (5)
b (Å)	13.484 (7)	12.602 (7)
c (Å)	32.291 (16)	13.527 (7)
α (°)	90.00	105.942 (4)
β (°)	90.438 (5)	106.788 (4)
γ (°)	90.00	100.777 (4)
Z	4	2
Volume (Å^3)	4489 (4)	1430.0 (13)
D_{calcd} (g/cm^3)	1.430	1.743
μ (mm^{-1})	1.646	2.549
F(000)	1984	752
Temperature	296(2)	293(2)
Crystal Size (mm)	0.20 × 0.20 × 0.18	0.25 × 0.22 × 0.20
Reflections Collected	24766	10288
Independent Ref. (R_{int})	8357 (0.0550)	5238 (0.0237)
Final R indices [I>2.0σ (I)]	R_1 = 0.0501	R_1 = 0.0258
	wR_2 = 0.0859	wR_2 = 0.0671
R indices (all date)	R_1 = 0.0841	R_1 = 0.0303
	wR_2 = 0.0978	wR_2 = 0.0698
GOF	1.032	1.011
Residual electron density(e Å^{-3})	–0.519 ~ 0.530	–1.262 ~ 0.682

Table S2 Selected Bond Lengths (Å), Angles (°) and Hydrogen Bonds for Complexes.

Tb-1

Tb(1)—O(3)	2.267 (4)	Tb(1)—O(5)	2.435 (4)	Tb(1)—O(11)	2.474 (5)
Tb(1)—O(4)	2.303 (4)	Tb(1)—O(7)	2.440 (4)	Tb(1)—O(10)	2.487 (4)
Tb(1)—O(14)	2.364 (4)	Tb(1)—O(8)	2.458 (4)	Tb(1)—O(13)	2.491 (4)
O(3)—Tb(1)—O(4)	96.05 (13)	O(14)—Tb(1)—O(8)	120.42 (15)	O(5)—Tb(1)—O(10)	116.80 (13)
O(3)—Tb(1)—O(14)	155.72 (16)	O(5)—Tb(1)—O(8)	132.46 (14)	O(7)—Tb(1)—O(10)	73.06 (15)
O(4)—Tb(1)—O(14)	77.78 (15)	O(7)—Tb(1)—O(8)	82.81 (16)	O(8)—Tb(1)—O(10)	51.11 (13)
O(3)—Tb(1)—O(5)	79.69 (14)	O(3)—Tb(1)—O(11)	125.12 (16)	O(11)—Tb(1)—O(10)	72.43 (15)
O(4)—Tb(1)—O(5)	73.89 (13)	O(4)—Tb(1)—O(11)	79.71 (15)	O(3)—Tb(1)—O(13)	74.30 (16)
O(14)—Tb(1)—O(5)	76.03 (16)	O(14)—Tb(1)—O(11)	77.35 (18)	O(4)—Tb(1)—O(13)	73.82 (14)
O(3)—Tb(1)—O(7)	79.38 (16)	O(5)—Tb(1)—O(11)	145.73 (14)	O(14)—Tb(1)—O(13)	124.78 (17)
O(4)—Tb(1)—O(7)	126.26 (15)	O(7)—Tb(1)—O(11)	145.01 (16)	O(5)—Tb(1)—O(13)	135.60 (14)
O(14)—Tb(1)—O(7)	85.44 (17)	O(8)—Tb(1)—O(11)	80.16 (16)	O(7)—Tb(1)—O(13)	148.70 (15)
O(5)—Tb(1)—O(7)	52.50 (14)	O(3)—Tb(1)—O(10)	122.57 (13)	O(8)—Tb(1)—O(13)	74.90 (15)
O(3)—Tb(1)—O(8)	76.52 (13)	O(4)—Tb(1)—O(10)	140.70 (13)	O(11)—Tb(1)—O(13)	51.77 (16)
O(4)—Tb(1)—O(8)	148.70 (14)	O(14)—Tb(1)—O(10)	69.56 (15)	O(10)—Tb(1)—O(13)	107.51 (15)

D—H···A	Distance (D—H)	Distance (H···A)	Distance (D···A)	Angles (D—H···A)
O(1)—H(1)···N(1)	0.8200	1.9400	2.670(7)	148.00
O(14)—H(1W)···O(15)	0.80(5)	1.93(5)	2.717(8)	170(8)
O(14)—H(2W)···O(13)^{i}	0.79(3)	2.05(3)	2.827(6)	168(5)

Symmetry code i: $-x+2, y+1/2, -z+1/2$.

Tb-2

Tb(1)—O(3)	2.300 (2)	Tb(1)—O(4)	2.449 (3)	Tb(1)—O(10)	2.465 (3)
Tb(1)—O(2)	2.312 (3)	Tb(1)—O(6)	2.421 (3)	Tb(1)—O(7)	2.511 (3)
Tb(1)—O(13)	2.346 (3)	Tb(1)—O(9)	2.445 (3)	Tb(1)—O(12)	2.583 (3)

O(3)—Tb(1)—O(2)	82.35 (10)	O(13)—Tb(1)—O(4)	76.18 (10)	O(6)—Tb(1)—O(7)	69.95 (11)
O(3)—Tb(1)—O(13)	155.77 (10)	O(6)—Tb(1)—O(4)	52.04 (10)	O(9)—Tb(1)—O(7)	51.13 (10)
O(2)—Tb(1)—O(13)	86.08 (11)	O(9)—Tb(1)—O(4)	123.16 (10)	O(4)—Tb(1)—O(7)	117.81 (11)
O(3)—Tb(1)—O(6)	85.62 (11)	O(3)—Tb(1)—O(10)	77.12 (10)	O(10)—Tb(1)—O(7)	73.75 (11)
O(2)—Tb(1)—O(6)	129.34 (10)	O(2)—Tb(1)—O(10)	80.97 (11)	O(3)—Tb(1)—O(12)	124.58 (9)
O(13)—Tb(1)—O(6)	85.39 (12)	O(13)—Tb(1)—O(10)	121.96 (10)	O(2)—Tb(1)—O(12)	74.73 (9)
O(3)—Tb(1)—O(9)	125.24 (10)	O(6)—Tb(1)—O(10)	142.86 (11)	O(13)—Tb(1)—O(12)	71.87 (9)
O(2)—Tb(1)—O(9)	145.50 (10)	O(9)—Tb(1)—O(10)	85.53 (11)	O(6)—Tb(1)—O(12)	146.30 (10)
O(13)—Tb(1)—O(9)	74.46 (11)	O(4)—Tb(1)—O(10)	150.69 (10)	O(9)—Tb(1)—O(12)	72.26 (10)
O(6)—Tb(1)—O(9)	77.96 (11)	O(3)—Tb(1)—O(7)	74.14 (10)	O(4)—Tb(1)—O(12)	138.55 (10)
O(3)—Tb(1)—O(4)	80.55 (9)	O(2)—Tb(1)—O(7)	148.57 (10)	O(10)—Tb(1)—O(12)	50.12 (9)
O(2)—Tb(1)—O(4)	77.43 (9)	O(13)—Tb(1)—O(7)	123.13 (11)	O(7)—Tb(1)—O(12)	101.72 (10)

D—H···A	Distance (D—H)	Distance (H···A)	Distance (D···A)	Angles (D—H···A)
O(13) —H(1W)···O(12)^{i}	0.82(5)	2.11(5)	2.929(5)	179(7)
O(13)—H(2W)···N(1)^{j}	0.93(8)	1.84(8)	2.754(6)	171(7)

Symmetry code i: –x+1, –y, –z; *j*: –x+1, –y+1, –z.

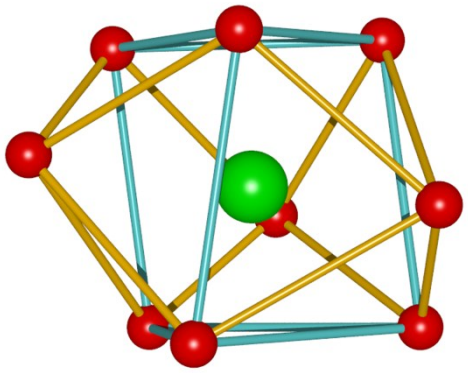

Fig. S1. Coordination polyhedron of the Tb^{3+} ion in **Tb-1**. O red, Tb green.

3. The XRD Pattern.

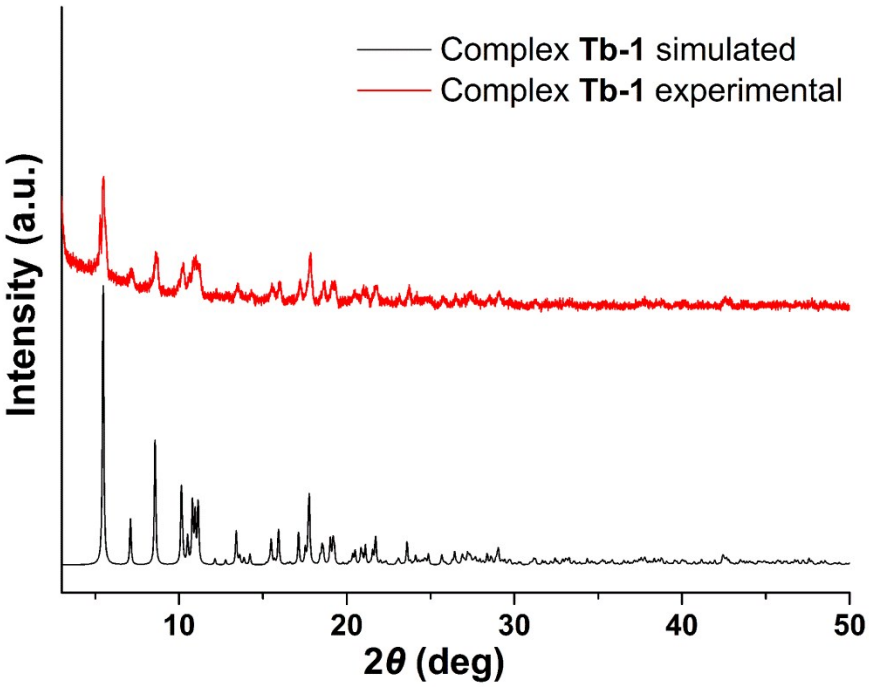

Fig. S2. PXRD patterns of simulated result from crystal complex **Tb-1** and experimental result.

4. UV-vis Absorption and Emission Spectra.

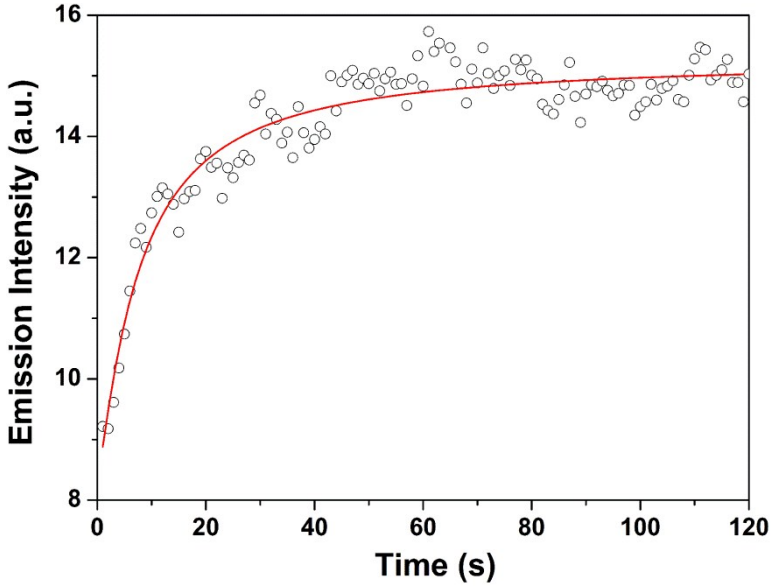

Fig. S3. The luminescence change of **Tb-1** monitored at 546 nm over time in the presence of Pb^{2+} ion in acetonitrile. [**Tb-1**] = 10 μM, [$Pb(ClO_4)_2$] = 50 μM, λ_{ex} = 360 nm.

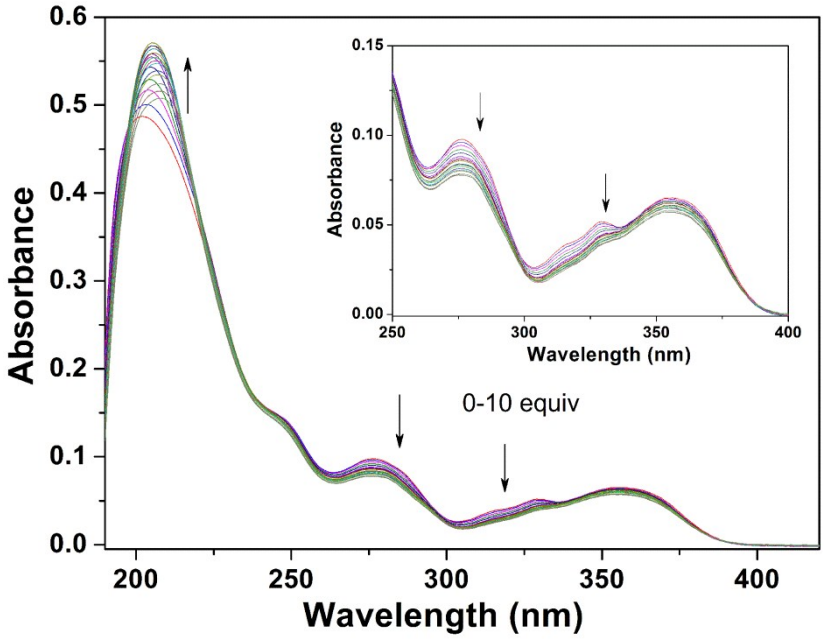

Fig. S4. The UV-vis absorption change of **Tb-1** upon addition of Pb^{2+} (0-10 equiv) in acetonitrile at room temperature. [**Tb-1**] = [Et_3N] = 10 μM.

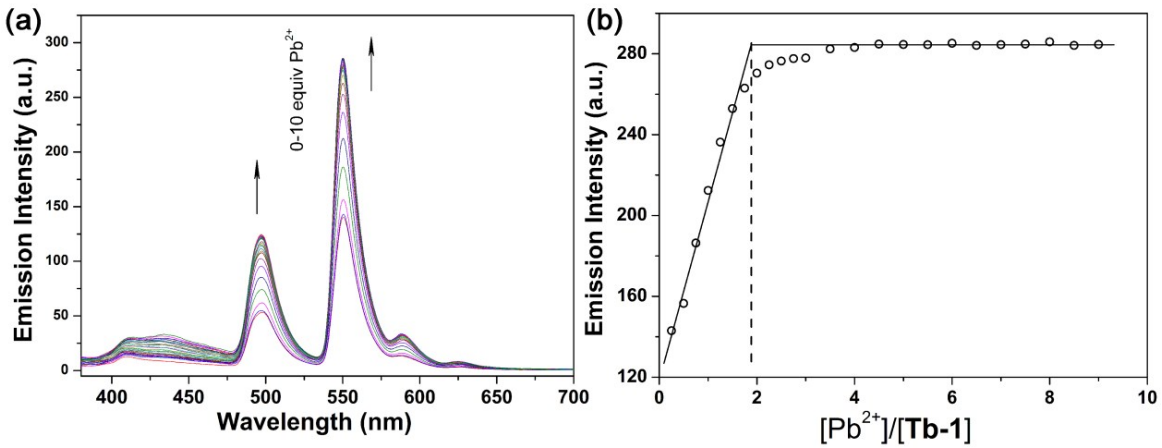

Fig. S5. (a) The steady-state luminescent spectra change of **Tb-1** upon addition of Pb^{2+} (0-10 equiv) in acetonitrile at room temperature. (b) The steady-state luminescent intensity at 546 nm as a function of [Pb^{2+}]/[**Tb-1**]. [**Tb-1**] = [Et_3N] = 10 μM, λ_{ex} = 360 nm.

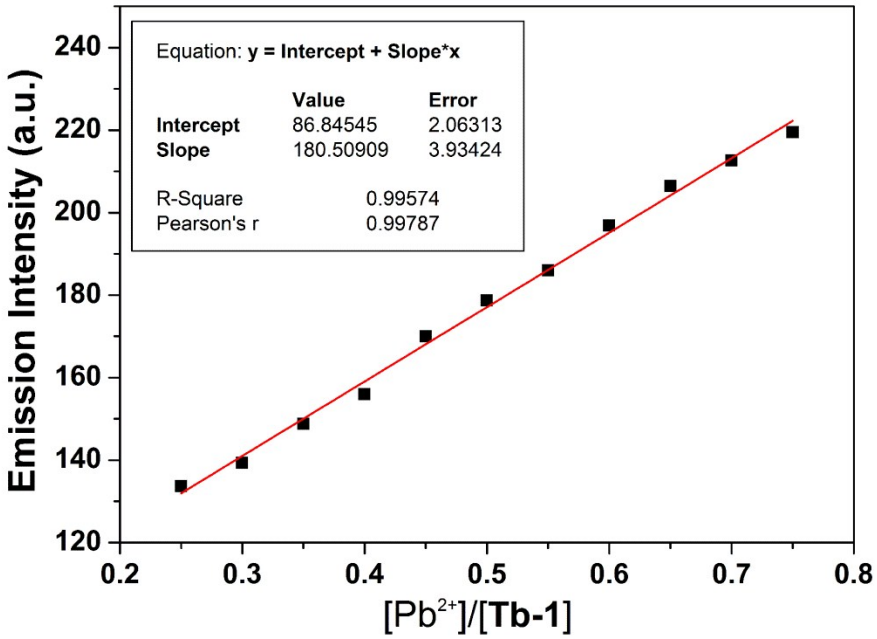

Fig. S6. The linear changes of luminescence intensity of **Tb-1** at 546 nm upon titration with Pb^{2+} in acetonitrile at room temperature. [**Tb-1**] = [Et_3N] = 10 μM, λ_{ex} = 360 nm.

The limit of detection (LOD) for Pb^{2+} was calculated by the linear function in Fig. S6 and the following equation:

$$LOD = \frac{3\sigma}{k} \times 10^{-5} \, (mol \cdot L^{-1})$$

Where σ is the standard derivation of luminescence intensity of 20 blank solutions; k is the slope of the linear calibration curve in Fig. S6 (180.5); the concentration of **Tb-1** is 1×10^{-5} mol·L^{-1}.

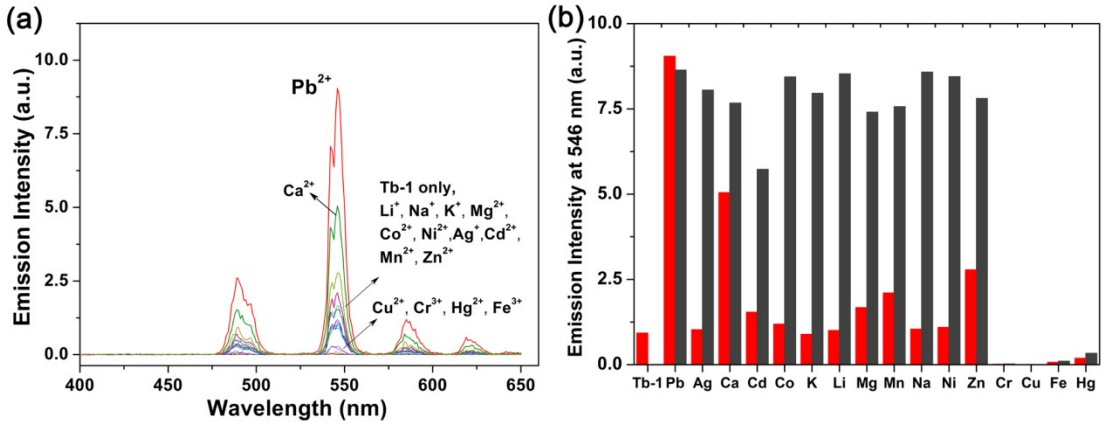

Fig. S7. (a) Time-gated luminescence spectra of **Tb-1** upon the addition of 5 equiv of various metal ions (Li^+, Na^+, K^+, Mg^{2+}, Ca^{2+}, Cr^{3+}, Mn^{2+}, Fe^{3+},Co^{2+}, Ni^{2+}, Cu^{2+}, Zn^{2+}, Cd^{2+}, Ag^+, Hg^{2+} and Pb^{2+}) in acetonitrile. (b) Relative luminescence intensities of **Tb-1** in acetonitrile at 546 nm: red bars represent addition of 5 equiv of various metal ions, and gray bars represent addition of 5 equiv of Pb^{2+} and 5 equiv of various metal ions to the solution. Time delay 0.05 ms, [**Tb-1**] = [Et_3N] = 10 μM, λ_{ex} = 360 nm.

5. IR Spectra.

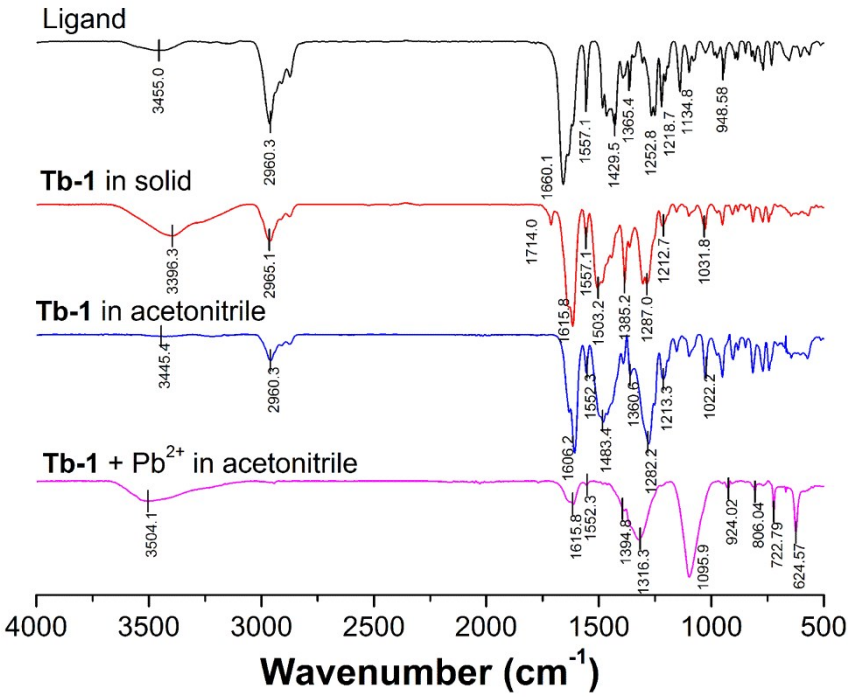

Fig. S8. IR spectra of the ligand, complex **Tb-1** in solid and in acetonitrile, and Pb^{2+}-induced hydroxide nanoclusters in acetonitrile.

6. Crystal Structure of Tb-2.

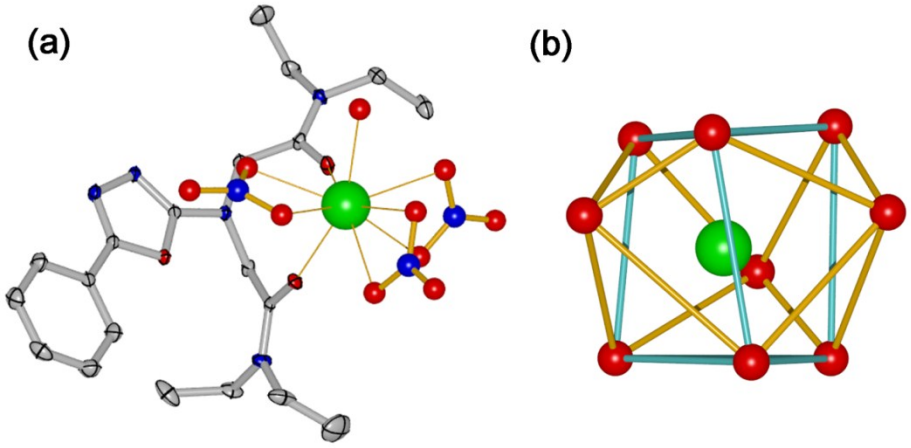

Fig. S9. (a) Crystal structure of **Tb-2**, in which Tb^{3+} ion is clamped by two amide groups and antenna group exhibits a planar structure. Hydrogen atoms and uncoordinated solvent molecule are omitted for clarity. Tb green, C gray, O red, N blue. (b) Coordination polyhedron of the Tb^{3+} ion in **Tb-2**. O red, Tb green.

7. The Phosphorescent Application of Chemosensor Tb-1.

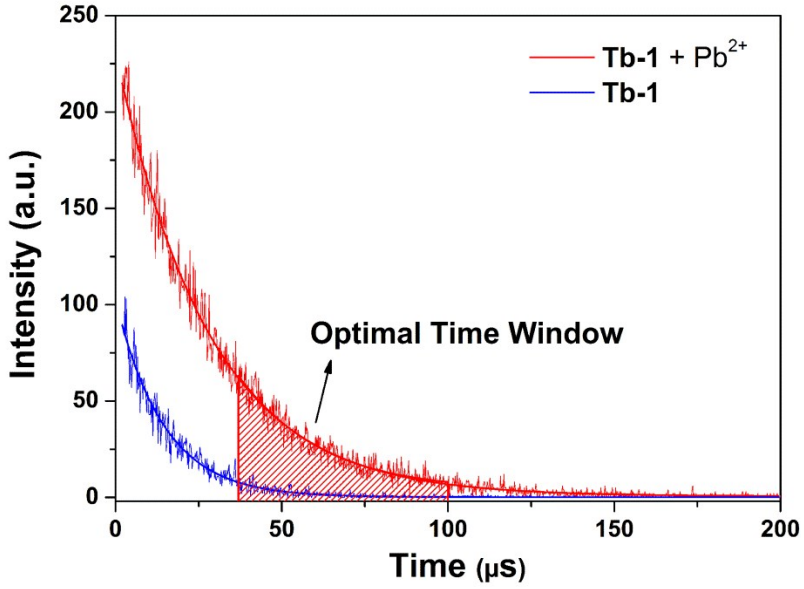

Fig. S10. Phosphorescence decay curves of **Tb-1** in the absence and presence of 5 equiv Pb^{2+} in acetonitrile at 546 nm. [**Tb-1**] = [Et_3N] = 10 μM, λ_{ex} = 360 nm.

8. The Charac

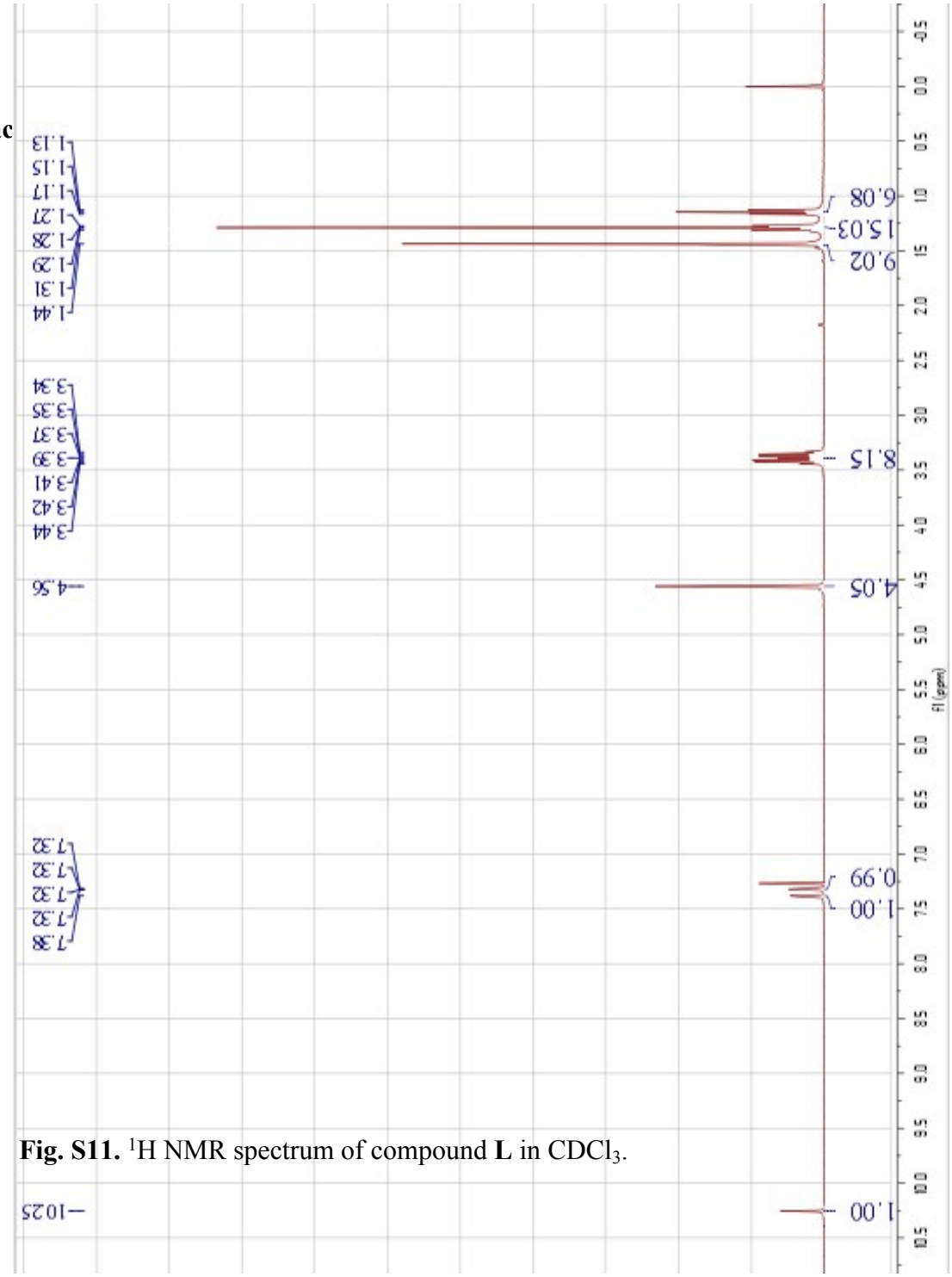

Fig. S11. ^{1}H NMR spectrum of compound **L** in $CDCl_3$.

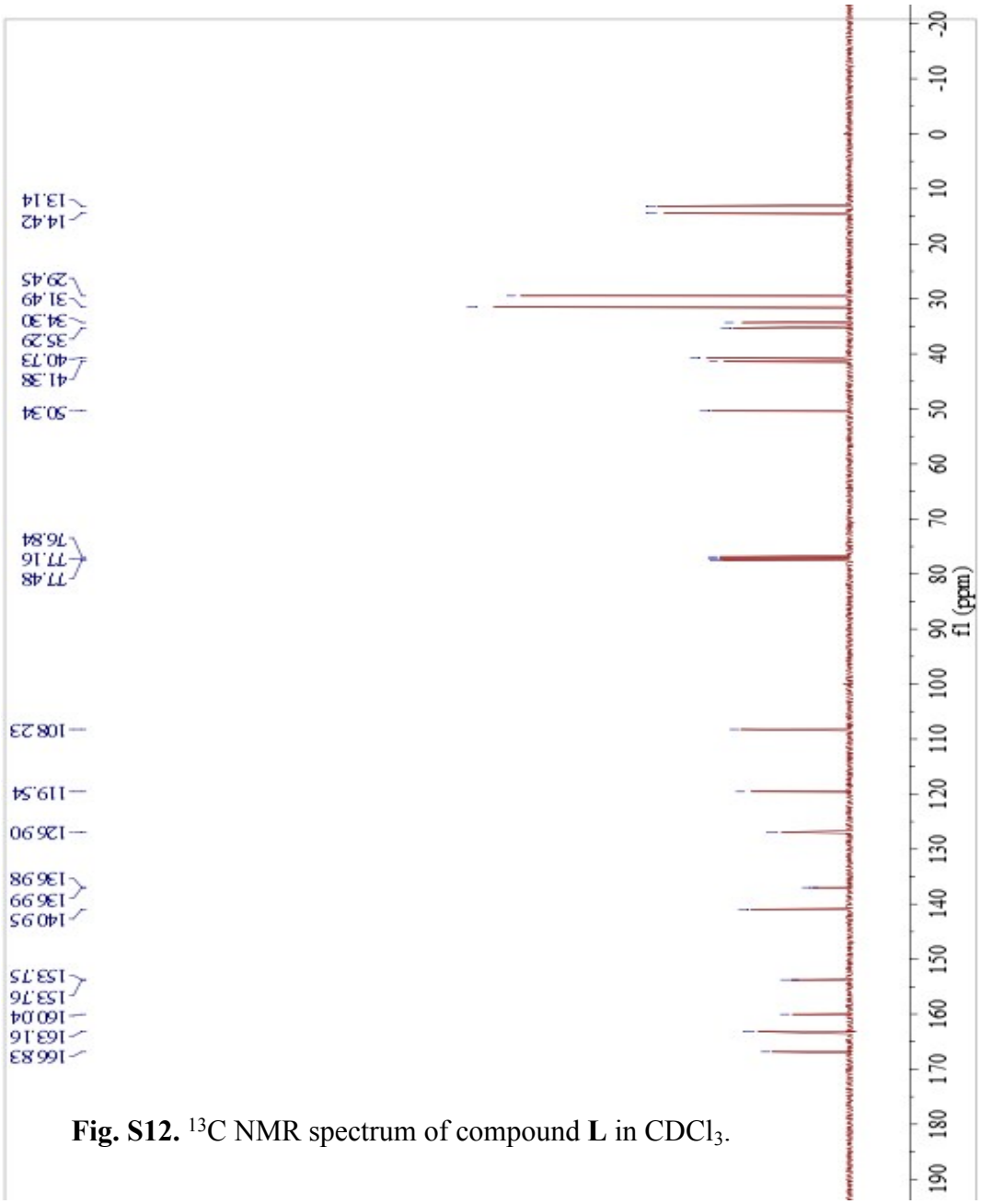

Fig. S12. ^{13}C NMR spectrum of compound **L** in $CDCl_3$.

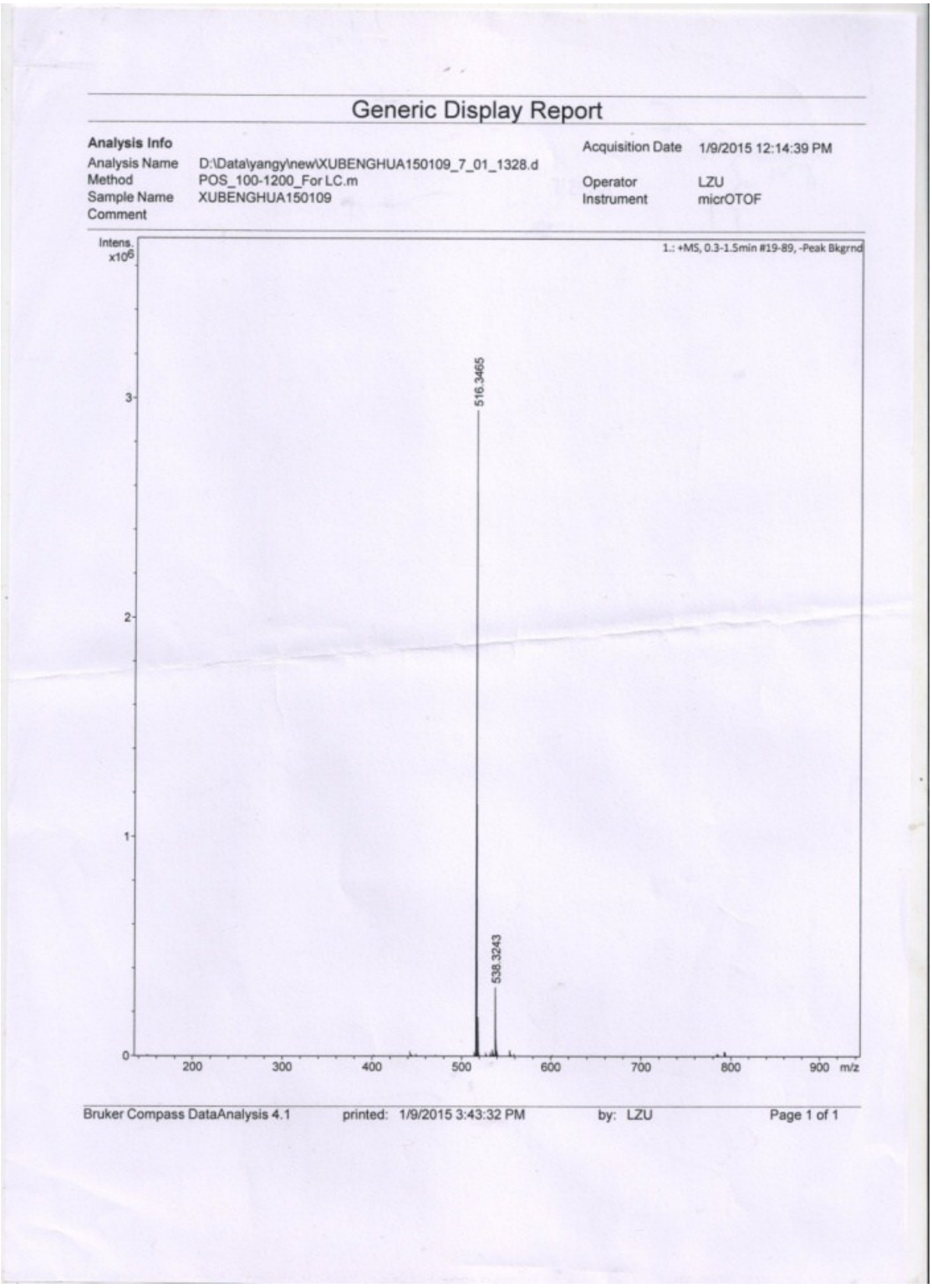

Fig. S13. ESI mass spectrum of compound **L**

REFERENCE:

1 J. A. Zhou, X. L. Tang, J. Cheng, Z. H. Ju, L. Z. Yang, W. S. Liu, C. Y. Chen and D. C. Bai, *Dalton Trans.*, 2012, **41**, 10626.